

Effects of Catalyst Pretreatment for Carbon Nanotube Growth

By

Caitlin D. Morgan

Submitted to the Department of Materials Science and Engineering on May 21st, 2007, in partial fulfillment of the requirements for the degree of Bachelor of Science in Materials Science and Engineering

Abstract

The effects of pretreatment of iron catalyst for carbon nanotube (CNT) growth was studied. CNTs were grown on Fe/Al₂O₃ (1/10 nm) thin-film catalyst deposited on silicon substrates via exposure to C₂H₄ in a thermal chemical vapor deposition (CVD) furnace. During CVD, the sample was exposed to a carrier gas (Argon) for the 35-minute temperature ramp, and 15-minute anneal, then to a mix of carrier gas and ethylene for a 15-minute growth stage. Experiments were performed varying the amount of oxygen contaminant in the carrier gas, and the time of hydrogen introduction. Samples were characterized via atomic force microscopy (AFM), scanning electron microscopy (SEM) and transmission electron microscopy (TEM). It was found that the later hydrogen was introduced, the higher the catalyst density and the taller the CNT carpet. The catalyst efficiency was also shown to increase with later hydrogen introduction. No clear trend was observed between the amount of oxygen in the carrier gas and the height of CNT growth. Data points to the model of catalyst coarsening being crucial to the nucleation and growth of CNTs and the parameters of CNTs grown. Variations in trends are discussed.

Thesis Supervisor: Carl V. Thompson

Title: Stavros Salapatas Professor, Department of Materials Science and Engineering

Co-Advisor: Gilbert D. Nessim

Table of Contents	Page
ABSTRACT	2
TABLE OF CONTENTS	3
LIST OF FIGURES	4
LIST OF TABLES	5
ACKNOWLEDGEMENTS	6
Chapter 1: Introduction	7
Chapter 2: Background Theory	
2.1 Carbon Nanotubes: Properties	8
2.2 CNT Growth Mechanism	9
2.3 Growth Methods	10
2.4 Effect of Hydrogen as a Reducing Agent	11
2.5 Methods of Characterization	12
Chapter 3. Experimental Methods	
3.1 Sample Preparation	14
3.2 CVD Furnace Setup	14
3.3 Gas Flows for Growth	15
3.4 Gas flows for AFM Series	16
3.5 Test of Argon contaminants	17
3.6 Characterization	17
Chapter 4: Results	
4.1 SEM Results for CNT Growth	19
4.2 TEM Results for CNT Growth	20
4.3 AFM Characterization of Iron Catalyst	21
4.4 SEM Characterization of Argon-Purity Study	23
Chapter 5: Discussion	
5.1 Best Growth Conditions as Seen via Electron Microscopy	25
5.2 Catalyst Morphology Determined via AFM	26
5.3 Oxidation States of Iron	26
5.4 Hypothesis	29
5.5 Explanation of Argon Study Results	32
Chapter 6: Conclusion	33
Chapter 7: Future Work	34
BIBLIOGRAPHY	36

List of Figures

Figure	Description	Page
1	CNT Schematic	8
2	Growth Cycle of CNTs	10
3	Furnace Setup	11
4	Coarsening	12
5	Furnace Setup	15
6	Growth Parameters	16
7	Images of CNT Carpet Growth	19
8	AFM Results	22
9	Height v Exposure to Hydrogen	22
10	AFM of Alumina-only samples	23
11	Ellingham Diagram Showing Iron Oxides	28
12	Iron-Oxygen Phase Diagram	29

List of Tables

Table	Description	Page
1	TEM Results	21
2	Argon Test Results	24

Acknowledgements

I would like to thank my advisors, Professor Carl V. Thompson and Gilbert D. Nessim, for their help and guidance in this project. Also, thanks to A. J. Hart, Nicola Abate, and Matteo Seita for their discussions.

Many thanks to Timothy and Cynthia Morgan for all of their support.

Chapter 1

Introduction

Carbon nanotubes (CNTs) are thin sheets of rolled graphene with high electronic and thermal conductivity and five times the strength of steel. Exact values depend on dimensions and chirality, and can vary widely with different growth parameters or methods. Such properties have long-since led to large amount of research. Aluminum and copper were previously used as interconnects, but at small scales, their resistivity is too high and limits devices.¹ Now, as the size of electrical devices is shrinking to a dimension approaching 45 nanometers, standard copper interconnects are projected to fail.² A replacement material is needed, and CNTs have been pinpointed as a possible new material for interconnects. CNTs are also being considered for use in sensors, field emission displays and transistors.

Currently, CNTs are not widely used in industry, largely because the growth mechanism is still unknown. Without this information, it is difficult to understand which growth processes will create nanotubes with the desired properties. Much research is underway to attempt a solution to this problem. Our study examines CNTs grown on an iron catalyst on an insulating substrate via thermal chemical vapor deposition (CVD). This allows us to easily examine the height and properties of CNT carpet growth. Here we compare the growth achieved with the morphology of the catalyst when a reducing gas is introduced at various times in the growth process. From this data, we hypothesize the optimal conditions for CNT growth and catalyst efficiency.

Chapter 2

Background Theory

2.1 Carbon Nanotubes: Properties

Carbon nanotubes (CNTs) were discovered in 1991 by Iijima.³ They are defined as thin sheets of rolled graphene, and are based on a hexagonal lattice of carbon atoms. CNTs can grow in many different ways, and exhibit extremely different properties. The diameter of a CNT has a large impact on its properties, and can vary up to 100 nm.

CNTs have excellent thermal conductivity, and are thermally stable.

Mechanically, CNTs are extremely strong.

CNTs can be multi-walled (MWCNTs) or single-walled (SWCNTs). MWNTs are a series of concentric rolled graphene sheets, exhibiting the band width of a semimetal, whereas SWNTs exhibit the electrical properties of a semiconductor or a metal, making them more versatile for different applications.

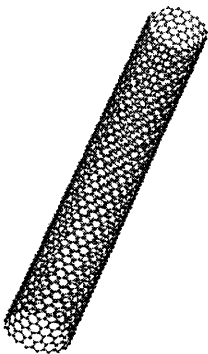


Figure 1. CNT Schematic.⁴

The chirality, or asymmetry of CNTs also has a large effect on their properties. Generally, when the sum of chiral vectors is a factor of three, the nanotube will exhibit metallic properties, otherwise it will perform as a semiconductor.⁵

Ability to align CNTs is important for their eventual use in the semiconductor industry. Currently, much growth on substrates leads to spaghetti-like clusters of CNTs with no apparent ordering. Dense, vertically aligned carpets of nanotubes are wanted for electronics applications; therefore achieving such carpets is an important parameter in CNT research.

2.2 CNT Growth Mechanism

While the growth mechanism for CNTs is yet unknown, a model has been proposed. In this model, according to Hofmann et al, there are four stages to CNT growth. The first is the adsorption of a carbon-carrying gas precursor molecule onto the catalyst, followed by the dissociation of said precursor. Next, the growth species diffuses into the catalyst. Finally, nucleation occurs and carbon begins to incorporate itself into the growing nanotube structure. When ethylene is used as a carbon source in a chemical vapor deposition (CVD) system, the third step, diffusion into the catalyst, is often the rate-limiting part of CNT growth. This is due to the fact that ethylene decomposition produces amorphous carbon, which tends to block the catalyst from being available to react with the precursors of a CNT.⁶ Dissociation of precursor molecules can also be rate-limiting, but we attempt to solve that problem by preheating the gasses in a three-zone furnace before reaching the sample.

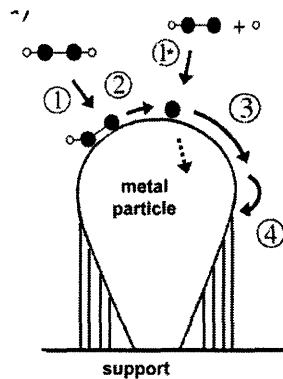


Figure 2. Growth cycle of CNTs.⁶ A diagram of the proposed growth mechanism of carbon nanotubes

CNT growth can happen in two different modes, depending on the catalyst/substrate system used. Tip growth, when new carbon atoms join the top of the growing CNT, has been shown to occur with certain catalysts, such as nickel. When an iron catalyst is used, the result is usually base growth, where new carbon atoms add to the nanotube at the base of the catalyst. Our catalyst/substrate system leads to base growth.

2.3 Growth Methods

Many methods are used for growing CNTs. Plasma enhanced CVD, thermal CVD, laser ablation, and arc discharge are some of the available methods. In this study, thermal CVD was used.

Thermal CVD has many benefits over other methods. Arc discharge and laser ablation do not allow for as much control over growth as CVD methods, and do not grow CNTs on a substrate. Plasma enhanced CVD leads to successfully controlled growth, but

is known to generate radicals that can etch away thinner nanotubes, leaving only thick, multi-walled tubes.⁷

In thermal CVD, the gasses are heated, causing them to decompose. The three-zone furnace used in this study allows for heating and decomposition to occur well before reaching the substrate. Thermal CVD allows CNTs to grow in-place, which makes it a suitable technique for semiconductor applications.

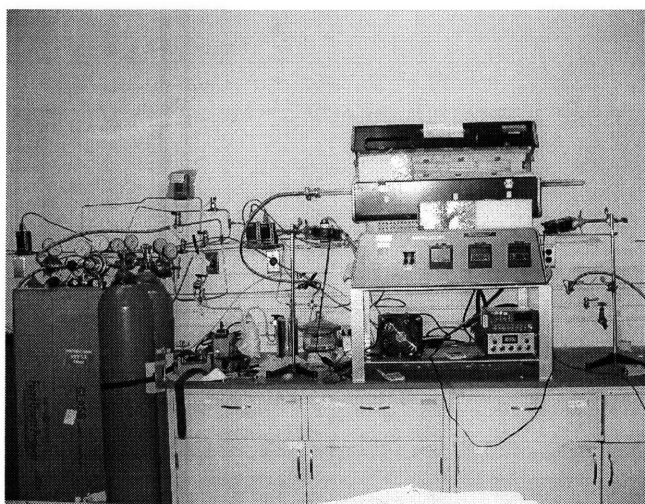


Figure 3. Furnace Setup. Digital Image of the furnace setup, with the furnace open, cooling for use.

2.4 Effect of Hydrogen as a Reducing Agent

Hydrogen, oxygen or water are often used as reducing or oxidizing agents in CVD growth of nanotubes. Water is only introduced in parts per million via gas contamination and recombination between oxygen and hydrogen. The addition of hydrogen as a reducing agent to the mix of gasses in a CVD furnace has been shown to effect the resulting CNT growth. We hypothesize that this is due to the fact that hydrogen reduces the catalyst to its metallic iron state. If the catalyst is in this state, coarsening can occur at high temperatures.⁸ However, if the catalyst is still oxidized, coarsening will not occur at

the growth temperature. Theoretically, the longer the catalyst is exposed to hydrogen, the coarser the catalyst particles will be. This theory is confirmed in this study via AFM morphology data.

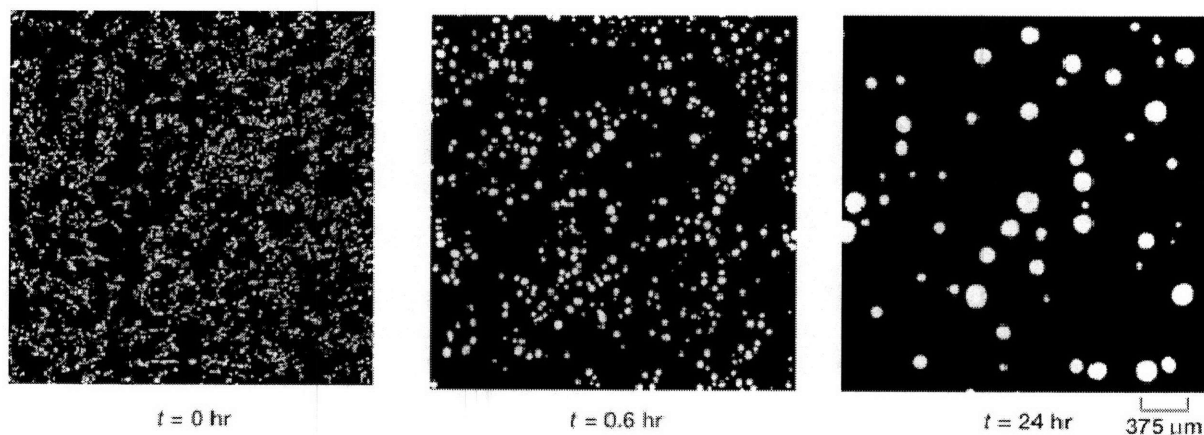


Figure 4. Coarsening. Demonstration of the coarsening of tin over a 24-hour period. Iron shows similar results.⁹

Optimized coarsening leads to the improved growth of nanotubes. With a coarsened catalyst, higher, more uniform carpets are shown to appear. The growth rate and catalyst efficiency are also shown to increase rapidly when coarsening occurs. Data shows that CNT diameter is proportional to catalyst size. Catalyst size is a direct result of coarsening, which is affected by hydrogen introduction. The morphology of the catalyst is therefore shown to impact the growth of nanotubes.

2.5 Methods of Characterization

CNT carpets may be characterized using a variety of methods. Given their nanometer scale, electron microscopy is especially useful. Scanning electron microscopy (SEM) can be used to determine the height, orientation, and relative density of a CNT carpet. Transmission electron microscopy (TEM) is useful for measuring the number of walls a CNT has, the inner and outer diameter of those walls. It is also useful to

characterize the catalyst used to grow CNTs. Atomic force microscopy (AFM) can give an indication of catalyst morphology, specifically the size, height, and density of catalyst particles formed during the anneal. XPS is useful in determining the oxidation state of the catalyst, however as this is usually performed *ex-situ*, it must be noted that the catalyst could have changed state. Together, this information can give a clear picture of carbon nanotubes, catalyst morphology, and, potentially, the oxidation state of the catalyst. A collection of this data can help to explain the growth mechanism of CNTs.

Chapter 3

Experimental Methods

3.1 Sample Preparation

Our study began with a 6-inch (100) silicon wafer (p-type 1-10 cm, Silicon Quest International). This was cleaned in a piranha solution (3:1 H₂SO₄:H₂O₂). Then 10 nm of Al₂O₃ and 1.2 nm of iron were deposited via e-beam evaporation without breaking vacuum. Deposition was done using a Temescal VES-2550 and an FDC-8000 film-deposition controller. Rutherford backscattering showed that the alumina had a high oxygen content rather than being stoichiometric. For CVD experiments, approximately 0.5 cm by 0.5 cm samples were cut from this wafer. Samples with only alumina deposited were also made, to be used as a reference in our AFM studies.

3.2 CVD Furnace Setup

A three-zone CVD furnace (Lindberg/Blue, model 59744-A) was used for all growth experiments. Each zone is nine inches long and had an individual thermocouple. A 2.25-diameter quartz tube was placed in the furnace and insulated at both ends. Tube length varied, but was roughly 100 cm long, allowing for samples to be removed from the furnace for rapid cooling before being exposed to air.

One end of the quartz tube was connected to gas canisters via mass flow controllers. This study utilizes three different purity grades of argon, as well as ethylene and hydrogen. The other end of the quartz tube was connected to a water bubbler in a fume hood.

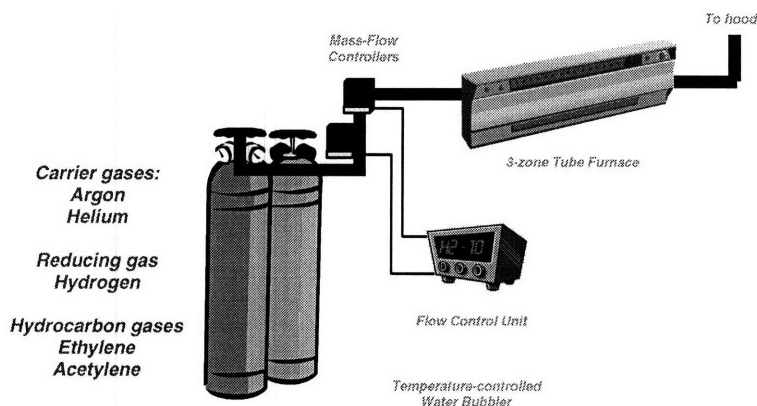


Figure 5. Furnace setup. The arrangement of a 3-zone thermal CVD furnace with gasses for CNT growth.

Samples were loaded in the furnace zone farthest from the start of gas flow, allowing gases to be preheated before reaching the sample. All samples were held on a 15-degree inclined quartz ramp in order to correct for nonuniformity of gas kinetics often observed in CVD systems. All gasses used were above 99.5% purity (research grade) unless specifically stated.

3.3 Gas Flows for Growth

Each experiment began with a 20-minute purge of the furnace with 600 standard cubic centimeters per minute (sccm) of argon, in order to evacuate any contaminants from the system. The furnace typically started with each thermocouple reading approximately 20°C. The temperatures were then increased to 755°C in the two zones farthest from the gas sources. The first zone remained unheated. This ramp period continued to have a gas flow of 600 sccm of argon, and lasted for 35 minutes. This was followed by a 15-minute anneal, still in only argon. Then, 150 sccm of ethylene was introduced into the system, beginning the growth phase of the cycle, which also lasted for 15 minutes.

400 sccm of hydrogen was introduced at various points during the growth cycle in order to test the effect of the introduction of a reducing agent on CNT carpet growth. Once hydrogen was added to the system, the argon flow rate was decreased to 200 sccm, so that the total flow rate for hydrogen and argon was maintained at 600 sccm. At the end of the growth phase, the furnace was shut down, but the sample remained inside for a slow cooling process. The furnace was opened at 650°C, and fans were used to cool the furnace once it reached 450°C. All cooling took place under argon flow.

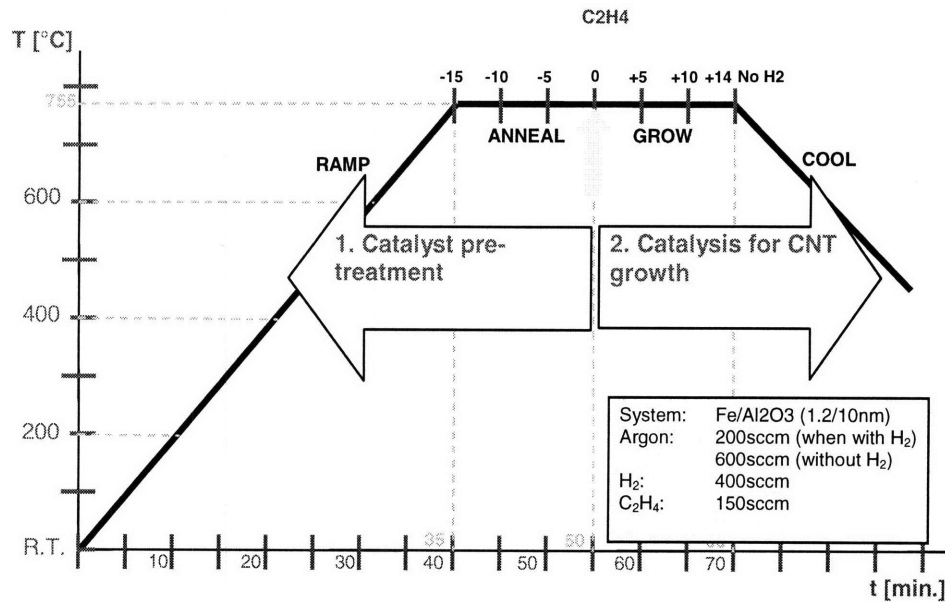


Figure 6. Growth parameters. The growth cycle examined in this study, consisting of a 35-minute ramp, 15 minutes of annealing at growth temperature, and 15 minutes of growth.

3.4 Gas Flows for AFM Series

As previous studies attempting to remove CNT carpets from the catalyst and then perform AFM characterization had failed due to sticking of the tip in residual growth, it was necessary to simulate growth in order to visualize the evolution of catalyst morphology versus time of hydrogen introduction. It has previously been shown that

ethylene dissociates into approximately 2/3 hydrogen, as well as other carbon-containing molecules.¹⁰ Therefore, to simulate growth, 100 sccm of hydrogen was introduced rather than 150 sccm of ethylene at the beginning of the growth stage for the experiments in this study. All other parameters remained the same. Rather than cooling slowly in the furnace, these samples were subjected to a fast-cool process outside the furnace to freeze catalyst, but still under argon. For this study, samples without catalyst films were also inspected as a reference for height.

3.5 Test of Argon Contaminants

It was hypothesized that the oxygen contaminant level in the carrier gas might be responsible for the change in CNT carpet height. In order to validate this theory, experiments were performed varying the grade of argon used as a carrier gas. Grades used were: high purity argon (parts per billion oxygen contaminant), argon contaminated with 100 ppm of oxygen, and standard research grade (ppm oxygen contamination) argon.

3.6 Characterization

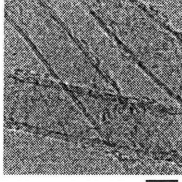
SEM analysis was done on growth samples and samples prepared to test the effect of oxygen contamination in argon. A high resolution JEOL 6320 was used in this characterization. Height, density, and alignment data was considered. TEM was performed on selected images in order to determine how many walls, average inner and outer diameter, growth rate, and areal density. Samples that were not exposed to ethylene were characterized via AFM (Digital Instruments Nanoscope IIIa / Dimension 3000

SPM), and the evolution of their morphology versus time of hydrogen introduction was studied.

Following this trend, it might be expected that introducing no hydrogen would lead to the best growth results, however when this was tried, the results were poor. There was little growth for the standard 15-minute growth time, although a carpet was achieved when the growth time was increased to 45 minutes. This implies that the introduction of hydrogen, or possibly another reducing agent, for at least a few minutes is crucial to the growth of carbon nanotubes in this system.

4.2 TEM Results For CNT Growth

TEM characterization was performed for representative samples during selected points in the growth cycle. It was found that later hydrogen introduction led to longer CNT length, smaller diameter, fewer number of walls, and larger areal density of CNTs. Introduction of hydrogen ten minutes after the start of growth gave the best results, with 0.9 mm tall carpets with a 7.4 nm average diameter, having on average 3 walls and an areal density of 4.9×10^{10} CNTs/cm². While these statistics are good, the areal density is an order of magnitude lower than the best available CNT density, reported by Fujitsu in November 2006.¹¹



H₂ introduced simultaneously with C₂H₄

~0.6mm
 9.8 ± 1.8 nm
 4.7 ± 1.0
 2.6×10^{10} cm⁻²
 ~60nm
 6.48×10^{10} cm⁻²

CNT Length
 CNT Diameter
 Number of Walls
 CNT Areal Density
 CNT Spacing
 Catalyst Density

H₂ introduced 10 minutes after C₂H₄ introduction

~0.9mm
 7.4 ± 1.0 nm
 3.0 ± 0.9
 4.9×10^{10} cm⁻²
 ~45nm
 7.5×10^{10} cm⁻²

Table 1. TEM Results

From A. J. Hart (top image is hydrogen introduction at start of growth, bottom image is hydrogen introduction 10 minutes after the start of growth)

4.3 AFM Characterization of Iron Catalyst

AFM characterization of as-is samples with iron catalyst showed an extremely flat surface. As seen in figure 7, when the sample was only exposed to argon, no change in morphology was observed. However, when hydrogen was introduced at the beginning of the experiment, small, closely-packed catalyst dots were seen. When hydrogen introduction occurred at 400°C, the catalyst particles were much larger, and there were barely any particles present. This is concurrent with previous work.¹² When hydrogen was introduced ten minutes before the start of growth, there were more smaller particles, although the density wasn't as high as when hydrogen was introduced at the start of the experiment. Introducing hydrogen at various points during the growth stage show smaller, closely packed catalyst particles. Height data shows that the height of catalyst particles increases with time of hydrogen exposure, indicating that coarsening is strongly affecting the catalyst morphology.

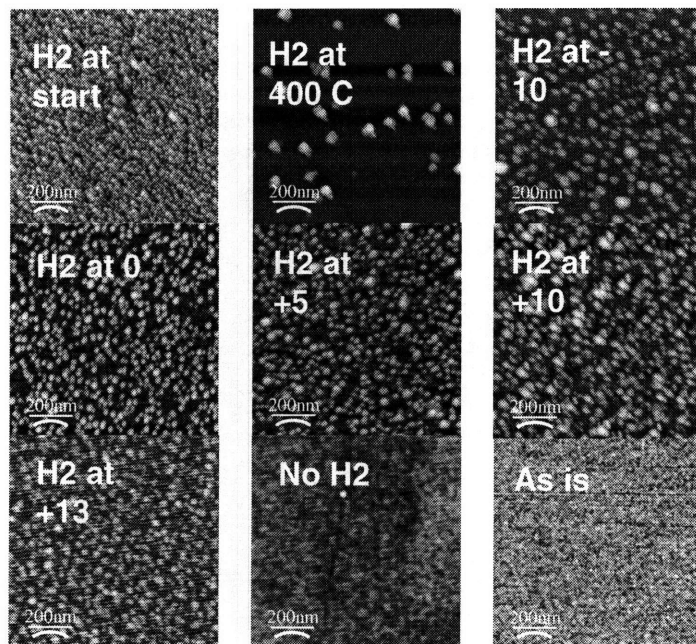


Figure 8. AFM Results. AFM data for samples taken at intervals along the growth study. Note coarsening effect of longer hydrogen exposure.

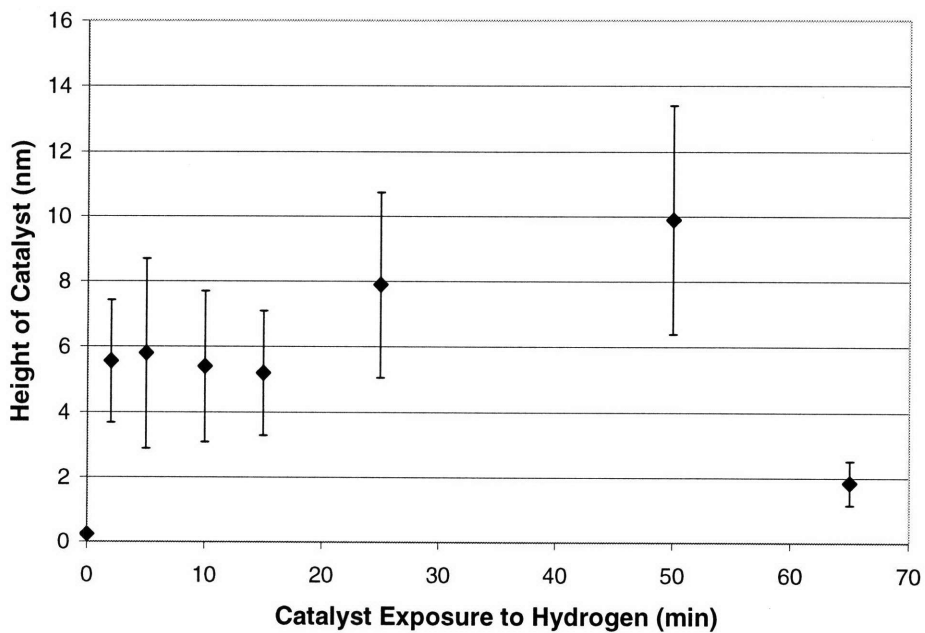


Figure 9. Height of Catalyst Versus Exposure to Hydrogen. Coarsening shown in this diagram. Hydrogen from start (65 minutes of exposure) requires further explanation.

Images of alumina-only samples showed no change in surface morphology throughout the cycle (Fig. 10). This contradicts previously reported data.¹³ Also, images

taken in the center and at the edges of samples showed no visible difference in morphology, in contrast with previous studies in this area.¹⁴

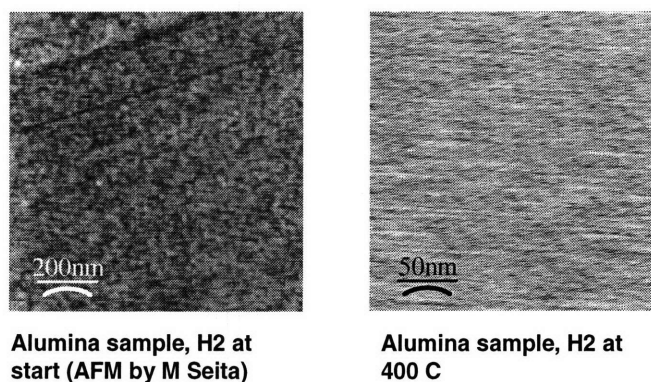


Figure 10. AFM of alumina-only samples. This shows that changes in morphology are due to changes in the catalyst, not the alumina layer.

4.4 SEM Characterization of Argon-purity Study

SEM analysis of CNT carpet height was performed on samples using three grades of argon purity. In the sample where hydrogen was introduced at the beginning of the ramp, low-oxygen or standard argon gave a carpet of approximately 0.5 mm, while no growth was achieved with high-oxygen argon. When hydrogen was introduced when the furnace reached 400C, all argon types failed to produce a carpet. In the case of hydrogen introduction ten minutes before the start of growth, all three argon types produced a carpet on the order of 0.4 mm, and when hydrogen was introduced at the start of growth, the carpet was roughly 0.5 mm for all samples. These results only show a difference when hydrogen is introduced at the beginning of the experiment, which is also the data point that clashes with the coarsening trend.

Sample	Visual inspection	SEM height (μm)
Low O ₂ , H ₂ @ start	Carpet	~ 550
Standard O ₂ , H ₂ @ start	Uniform carpet	~ 450
High O ₂ , H ₂ @ start	Growth in spots and edges	~100
Low O ₂ , H ₂ @ 400 C	Growth around edges	~ 50
Standard O ₂ , H ₂ @ 400 C	No visible thickness	< 10
High O ₂ , H ₂ @ 400 C	Very little growth in spots & edges	~ 60
Low O ₂ , H ₂ @ -10 min	Carpet	~ 400
<i>Standard O₂, H₂ @ -10 min</i>	<i>Almost uniform carpet & clusters</i>	~ 330
High O ₂ , H ₂ @ -10 min	Carpet	~ 500
Low O ₂ , H ₂ @ 0	Carpet	~ 500
Standard O ₂ , H ₂ @ 0	Uniform carpet	~ 450
High O ₂ , H ₂ @ 0	Carpet	~ 565

Table 2. Argon Test Results. Variations in argon purity and their effect on CNT carpet height.

Chapter 5

Discussion

5.1 Best Growth Conditions (Hydrogen at +10 minutes)

Scanning electron microscopy shows the best CNT growth occurs when hydrogen is introduced at the end of the growth phase. CNTs are the highest, densest, and most vertically aligned. Earlier hydrogen introduction is also shown to produce vertically aligned CNTs (VACNTs) of hundreds of microns, but on closer inspection, the CNTs are less defined and less dense. Hydrogen introduction at the start of the experiment is the only point which is contrary to this trend. At this point, growth is very high and only slightly less dense and well-aligned than the best results. It is also shown that growth rate is greatly heightened by later hydrogen introduction, assuming growth without hydrogen introduction as a reference.

Data extrapolated from transmission electron microscopy shows that later hydrogen introduction leads to smaller, more dense nanotubes. Assuming the nanotube size scales with the catalyst particle size, this is consistent with the idea that longer presence of reducing agents leads to coarsening. The later hydrogen is introduced, the less coarsening occurs, and therefore nanotubes are smaller in diameter.

When compared to catalyst data obtained via AFM, TEM data showed that later hydrogen introduction led to improved catalyst efficiency. Catalyst efficiency was measured as the CNT areal density divided by catalyst particle density as calculated via TEM and AFM. This is based on the assumption that a catalyst particle produces one CNT. The maximum efficiency obtained, 60%, is quite good for thin-film catalysts,

almost as good as results obtained with nanoparticle catalysts.^{15,16} An explanation for this is attempted.

5.2 Catalyst Morphology Determined via AFM

As could be expected, catalyst coarsening is shown to generally increase with time of exposure to the reducing agent. However, there are a few notable exceptions which must be considered. The first is that when hydrogen is introduced at or after the start of growth, there is only a small increase in catalyst height. Before that point, catalyst dot height is shown to increase fairly rapidly with time of hydrogen introduction. A model is proposed of why this trend is not more linear.

The model also attempts to answer the question of why the experiment with hydrogen introduced at the beginning of the experiment is less coarse, rather than following the trend and being the highest, as exposure to hydrogen was the longest by several minutes. This point is puzzling, as this experiment has so far failed to follow other trends as well.

5.3 Oxidation States of Iron

The iron catalyst is known to have up to 16 oxidation states.¹⁷ We assume our catalyst to be oxidized before the start of our experiments, as they have been exposed to air for over one year. It has been shown that at low temperatures, Fe_2O_3 and Fe_3O_4 are the most stable oxide, and therefore the one formed most commonly.¹⁸ However, at 570°C , FeO becomes a stable oxide as well.¹⁹ Chemically, this is significant because FeO is much more difficult to reduce than Fe_2O_3 . As this temperature occurs during the growth

cycle examined here, this effect must be considered. However, as our system is constantly exposed to oxidizing agents via contamination, we make the assumption that our oxide remains in the Fe_2O_3 state, which is the most oxidized. Pure Fe is believed to be the catalyst for CNT growth.

There is one other important chemical point to consider. Hydrogen is known to begin to form water when mixed with oxygen at a temperature between 100 and 200°C.²⁰ While hydrogen is a reducing agent for iron, water is an oxidizing agent. Bearing both of these effects in mind, as well as growth results and catalyst morphology, a model is now given to attempt an explanation for CNT growth behavior as related to the introduction of hydrogen.

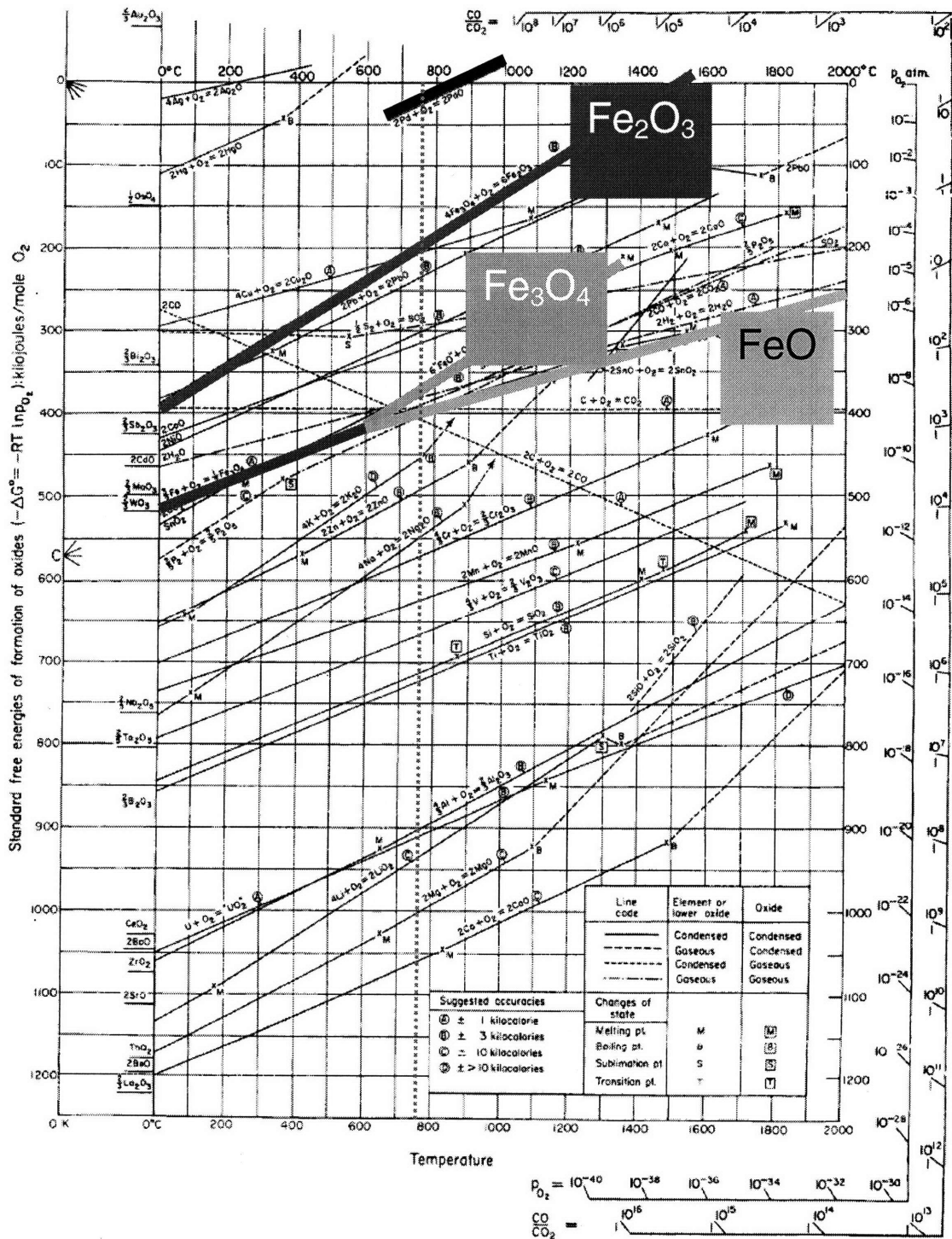


Figure 11. Ellingham Diagram Showing Iron Oxides. Shows the tendency for FeO, which doesn't reduce easily to form at higher temperatures.²¹

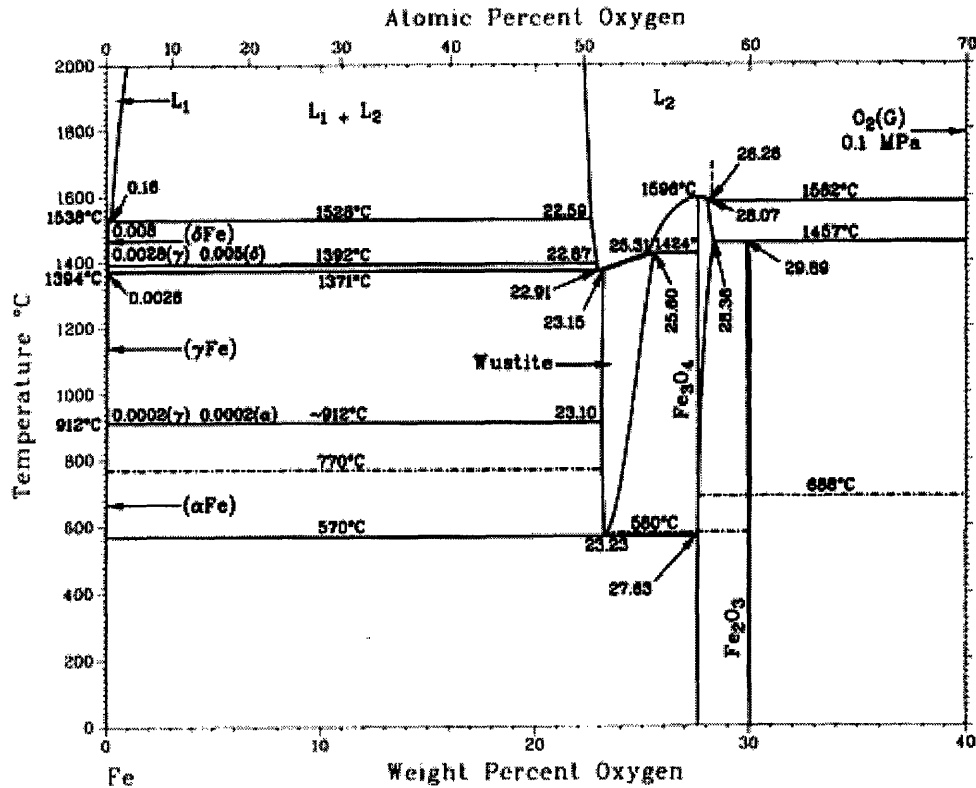


Figure 12. Iron-Oxygen Phase Diagram. Only temperatures below 800°C need be considered for this study.

5.4 Hypothesis

It has been shown²² that at above 570°C, Fe₂O₃ reduces to first Fe₃O₄, then FeO, and finally Fe. This is believed to occur almost spontaneously at temperatures as high as our growth temperature of 755°C. In this study, six points were examined with hydrogen introduction at this temperature, all of which produced growth. It was noted that the less time hydrogen was present in the system, the longer and denser the nanotubes were.

We will start comparing the two points in table 2, hydrogen introduction at the start of growth and ten minutes after. In the first case, growth occurred on metallic iron (Fe) that was fully reduced for 15 minutes and had no ethylene pretreatment (ethylene flow before hydrogen introduction). When hydrogen was introduced ten minutes after the

start of growth, the catalyst had been fully reduced for five minutes, and had been exposed to 10 minutes of ethylene pretreatment, which may have allowed for previous partial reduction due to decomposition into hydrogen.¹⁰

The effect of ethylene pretreatment on Fe thin-films is unknown. However, we attempt to show the differences in growth results in this regime as a difference in morphology. TEM and AFM show that coarsening occurs with longer hydrogen presence. It has been shown that carbon needs a certain amount of time for adsorption into the catalyst, an incubation period which delays the start of growth.^{23,24} This time is proportional to the size of the catalyst particles, increasing as the diameter of the catalyst increases.²² It is also possible, though uncertain, that the catalyst has a limited lifetime and doesn't survive for the entire growth period. This possibility, along with the incubation time, could explain why CNTs produced over longer growth times (of up to 15 minutes) are not as high as those produced with hydrogen-aided growth of only five minutes. This idea is supported by TEM and TGA data, which show that introducing hydrogen for less time dramatically increases the growth rate of CNTs.

During the ramp stage we observed lack of growth the introduction of hydrogen at 400°C, which can also be explained by a difference in morphology. At this point, we propose that the catalyst has been reduced and coarsening for such a large amount of time, that it becomes unsuitable for CNT growth. We are uncertain at this time whether this is due solely to morphology effects, or if there are other parameters to take into consideration.

Hydrogen introduction at the start has been the most difficult question to attempt an answer for. Some sources have found that hydrogen won't exhibit any reducing effect

on iron oxides at temperatures below 400°C.²⁵ Others, however, state that reduction does in fact occur at temperatures as low as 125°C, and that oxides reduced by hydrogen at such low temperatures will produce small Fe particles,²⁶ which we would expect to coarsen more as higher temperatures were achieved. However, our AFM data for this point, doesn't fit the coarsening trend. As of now, we are unable to explain this point, but propose that it cannot be due to morphology alone. Oxidation states may play a role in this point.

Something else to consider is the fact that even while reduction is taking place at the surface, oxidation is taking place simultaneously. Since we have only parts per million of oxygen and water in the gas bottles, this effect is the most important to consider at low temperatures, when hydrogen's reducing effect on iron oxides is low. When hydrogen is introduced from the start, water (a weak oxidizing agent) will form at the lowest temperature possible, when much of the oxide isn't yet reduced. This could lead to cycling of the sample between being oxidized and reduced until a higher temperature is reached. At higher temperature points, cycling should still occur, but may not be as effective, as we still begin with Fe₂O₃, which is reduced much more easily than it is oxidized, an effect that will be amplified at high temperatures. Also, in these systems, cycling doesn't occur until much later in the experiment, as only oxidizing agents are present until hydrogen is introduced. Researchers are currently very interested in the effect of multiple redox cycles on resultant Fe²⁺. Either of these two possible mechanisms (oxidation state changes or cycling) could prevent the final Fe from forming and coarsening until much later in the cycle.

5.5 Explanation of Argon Study Results

It remains very much in question why only the experiment with hydrogen introduction from the start was influenced by the oxygen content of the argon. Following the theory of coarsening the no-growth result achieved at start with high-impurity argon is what we would expect with the standard argon. As this is not the case, we propose again that morphology is not the key factor in this change. Again, we are unable to propose a solid model at this point, but suggest it relates to either an oxidation state, or the loss of the oxidation-reduction cycle hypothesized earlier.

Chapter 6

Conclusion

Our results show that oxygen contaminants in the carrier gas have little or no effect on the growth of CNT carpets when varied by many orders of magnitude. This pinpoints the effect of the reducing gas, hydrogen, as largely influencing CNT growth. Therefore, we studied the catalyst layer being reduced.

A model is proposed in which hydrogen reduces the iron catalyst, leading to higher coarsening. AFM morphology data, and electron microscopy data confirm this model. AFM images of the as-is catalyst, and catalyst annealed in argon with no hydrogen present further support this theory.

AFM data shows that the later hydrogen is introduced into the system, the higher the catalyst density. SEM shows that late hydrogen introduction also leads to the best growth. TEM and AFM show that this leads to high catalyst efficiency of up to 60%. This shows that the chemistry between the catalyst and hydrogen plays an important role in the production and properties of CNT carpets and can be altered to achieve CNTs of varying characteristics.

The one question remaining has to do with the sample where hydrogen is introduced at the start of the experiment. It leads to very high catalyst density and good CNT carpet height. While this is still under investigation, it is hypothesized that this is due to a different chemical atmosphere when reduction occurs at low temperatures. This is probably not affecting samples where hydrogen is introduced during the ramp stage. More work needs to be done in this area, and XPS results are suggested to help determine the catalyst oxidation state.

Chapter 7

Future Research

In the future, we propose to further the study of hydrogen's reducing effect on the catalyst in CNT growth. This could be studied by increasing the annealing time and again testing the results via AFM. Also, the oxidation state of the catalyst must be determined. This can possibly be done via in-situ XPS (we attempted ex-situ XPS and the results were difficult to interpret). This would help to explain why our sample with hydrogen introduced at start doesn't follow the trend, and could also explain poor growth results when hydrogen is introduced during the ramp or early anneal stage of our growth process.

Studies will also continue checking the effect of oxygen present in the carrier gas, this time by using titanium getters to help remove oxygen from the system. Helium and acetylene are also being tested as alternative carrier gasses and carbon sources. We are also planning to test the gas output of the furnace to determine if a specific component of ethylene decomposition causes or inhibits growth.

It was noted in our studies that the quartz tube used had a strong effect on the quality of CNT carpet produced. Namely, using a new tube led to poor or no growth, while the same experiment with an old tube, that was black due to carbon from previous experiments, gave good results. It was discovered that although we purchased fused quartz tubes, which should be amorphous, the middle section of the tube wasn't necessarily exposed to fusing temperatures (above 2000C).²⁷ This problem was

temporarily solved by being sure to always use the same tubes, but needs to be studied in the future.

Bibliography

-
- ¹ www.tf.uni-kiel.de/~kap_5/illustr/i5_4_1.html
- ² ITRS Roadmap 2004
- ³ Iijima S. 1991. *Nature*. 354. Pg 56-58.
- ⁴ <http://www.ewels.info/img/science/nanotubes/tube.angled.jpg>
- ⁵ Dresselhaus et al. *Physics World*. February 1998.
- ⁶ S. Hoffman et al. *Surface Diffusion: The Low Activation Energy Path for Nanotube Growth*. Physical Review Letters. 12 July 2005.
- ⁷ G. Zhang et al. *Ultra High-Yield Growth of Vertical Single-Walled Carbon Nanotubes: Hidden Roles of Hydrogen and Oxygen*.
- ⁸ Cantor et al. *Nanoletters*. 2006.
- ⁹ <http://www.grc.nasa.gov/WWW/RT2002/6000/6728hickman.html>
- ¹⁰ G. Towell et al. *Kinetic Data from Nonisothermal Experiments: Thermal Decomposition of Ethane, Ethylene, and Acetylene*. A.I.Ch.E. Journal. Vol. 7, No. 4, 1961.
- ¹¹ Sato et al. *Effect of Catalyst Oxidation on the Growth of Carbon Nanotubes by Thermal Chemical Vapor Deposition*. Journal of Applied Physics. 100. 2006.
- ¹² I. Sushumna et al. *Role of Physical and Chemical Interactions in the Behavior of Supported Metal Catalysts: Iron on Alumina- A Case Study*. Journal of Catalysis, 94. 239-288, 1985.
- ¹³ Chakrabarti et al. *Number of Walls Controlled Synthesis of Millimeter-Long Vertically Aligned Brushlike Carbon Nanotubes*. Journal of Physical Chemistry C. 22 November 2006.
- ¹⁴ J. Kim. *The Role of Hydrogen in the Growth of Carbon Nanotubes: A Study of the Catalyst State and Morphology*. MIT DMSE, 2006.
- ¹⁵ Don N. Futaba et al. *84% Catalyst Activity of Water-Assisted Growth of Single Walled Carbon Nanotube Forest Characterization by a Statistical and Macroscopic Approach*. 23 Feb. 2006. Physical Chemistry B.
- ¹⁶ M. Ishida et al. Japanese Journal of Applied Physics. 2004, 43, L1356.

¹⁷ Cornell, R. M.; Schwertmann, U., *The iron oxides : structure, properties, reactions, occurrences, and uses*. 2nd, completely rev. and extended ed.; Wiley-VCH: Weinheim, 2003; p xxxix, p. 664.

¹⁸ Nathalie Bertrand et al. *Low-Temperature Oxidation of Pure Iron: Growth Kinetics and Scale Morphologies*. Materials Science Forum volumes 461-464. 2004.

¹⁹ Kent R. Rhodes, Ph.D., McCrone Associates, Inc. Westmont, IL. *Analysis of Iron Oxidation States by XPS*.
<http://www.modernmicroscopy.com/main.asp?article=67>.

²⁰ A. Biela J. Haber, *Oxygen in catalysis*. New York: M. Dekker, 1991.

²¹ Gaskell, D. R., *Introduction to the thermodynamics of materials*. 4th ed.; Taylor & Francis: New York, 2003; p xv, page 618.

²² A. Pineau et al. *Kinetics of Reduction of Iron Oxides by H₂, Part I: Low Temperature Reduction of Hematite*. Thermochimica Acta, Vol 447, 2006, page 89-100.

²³ Ting et al. *Low-Temperature Nonlinear Rapid Growth of Aligned Carbon Nanotubes*. Chemical Physics Letters, vol 396, 2004. p 469-472.

²⁴ C. Dang et al. *Study on Effects of Substrate Temperature on Growth and Structure of Alignment Carbon Nanotubes in Plasma-enhanced Hot Filament Chemical Vapor Deposition System*. Applied Surface Science, vol 253, 2006. P 904-908.

²⁵ Pena et al. *Kinetic Study of the redox process for storing hydrogen: Reduction stage*. Catalysis Today, vol. 116, pp. 439-444, 2006.

²⁶ A. D. Franklin et al. *Low Temperature Reduction of Iron Oxides*. January 1955, Vol 59. pg 65-67.

²⁷ <http://www.unitedsilica.com/products/index.htm>